Scale-dependent shifts in demographic and environmental control of temporal β-diversity

Cristina M. Jacobi[1] & Tadeu Siqueira[1,2]

[1] Departamento de Biodiversidade, Instituto de Biociências, Universidade Estadual Paulista (UNESP), Rio Claro, SP, Brasil

[2] School of Biological Sciences, University of Canterbury, Private Bag 4800, Christchurch 8140, New Zealand, ORCID: 0000-0001-5069-290

Corresponding author: Tadeu Siqueira (tadeu.siqueira@unesp.br)

Author Contributions: CMJ and TS contributed equally to study conception and design. CMJ led data aquisition. CMJ and TS contributed equally to analysis and interpretation of results. CMJ wrote the first draft with substantial input from TS.

Abstract

Aim: We investigated whether the relative influence of demographic stochasticity and environmental forcing on compositional dynamics shifts across scales.

Location: Riverine fish communities sampled across 39 regions in three biogeographic realms.

Time period: 1981–2019.

Major taxa studied: Freshwater fish.

Methods: We first used simulations without environmental selection to assess whether temporal β-diversity metrics capture demographic variability independent of community sizes. We then analyzed 468 fish community time series, modeling local temporal β-diversity and regional temporal changes in spatial β-diversity as functions of community size, its temporal variability, species richness, rarity, and environmental variation and synchrony.

Results: Simulations showed that a rank-change metric was not intrinsically biased by community size. Empirical analyses revealed scale dependence in the processes shaping compositional temporal variability. Locally, smaller median community size and higher abundance fluctuations increased temporal β-diversity, consistent with stronger demographic stochasticity in small communities. Temperature seasonality emerged as the strongest climatic correlate of local temporal β-diversity, with more seasonal environments exhibiting greater inter-annual compositional change. Mean annual temperature and species richness also showed positive effects. In contratst, internal community properties did not predict regional dynamics. Instead, spatial synchrony of precipitation was the main predictor. More synchronized environments exhibited lower temporal variability in among-site dissimilarity, consistent with Moran-type environmental forcing constraining spatial β-diversity.

Main conclusions: Our findings reveal a scale-dependent shift in the processes shaping compositional dynamics, with demographic stochasticity and and climatic regime jointly

structuring local compositional dynamics, whereas environmental synchrony dominating regional variability. These findings link demographic and environmental perspectives, clarifying how biodiversity change propagates across scales under declining populations and increasingly variable climates.

Keywords: demographic stochasticity, ecological drift, community size, compositional variability, spatial scale, spatial synchrony, metacommunities

Introduction

Ecosystems show decreasing temporal variability when analyzed across broader spatial scales, higher organizational levels, or more complex trophic structures (Wang et al. 2019, Kéfi et al. 2019, Hammond et al. 2020, Rezende et al. 2021, Siqueira et al. 2024). This scaling pattern has been associated with multiple sources, including statistical averaging (Doak et al. 1998) as well as deterministic mechanisms such as compensatory species dynamics (Gonzalez and Loreau 2009), mobile predators (McCann et al. 2005) and spatially synchronized environmental effects (Steiner et al. 2013). Stochastic processes, particularly demographic stochasticity, are also expected to influence variability, especially where local population sizes are small (Lande et al. 2003). Yet we lack a clear understanding of how random demographic events at the individual and population level cascade into turnover in species composition through time, and how the relative influence of demographic and environmental processes reorganizes across spatial scales. This gap persists despite the growing recognition of stochastic processes in ecosystems (Vellend 2016, Leibold and Chase 2018) and the increasing need to understand biodiversity temporal dynamics under global change (Shimadzu et al. 2015, Magurran et al. 2019, Tatsumi et al. 2021, Dornelas et al. 2023).

Demographic stochasticity is chance variation in individual fates (births, deaths) whose relative influence increases as population size declines (Reed and Hobbs 2004, Melbourne and Hastings 2008). At the population level, these random events produce drift-like temporal trajectories (Lande 1993). When such dynamics occurs independently among localities it generates asynchronous population dynamics that, when scaled up, can result in relatively large within-site compositional turnover through time (high temporal β-diversity) and also in high among-site dissimilarity in snapshot surveys (Siqueira et al. 2020, Jacobi and Siqueira 2023). Thus, compositional turnover metrics summarize the community-level

expression of these dynamics, providing a scalable, indirect signal of demographic drift rather than directly estimating species-level variance.

Environmental stochasticity (i.e., temporal variation in abiotic or biotic conditions) differs qualitatively from demographic noise because it can affect many individuals simultaneously (Lande et al. 2003). These processes leave different empirical signatures. Whereas demographic stochasticity generates uncorrelated, site-specific random walks in abundance (Melbourne and Hastings 2008), environmental stochasticity can produce synchronized temporal responses across sites if the driver is spatially correlated (Bjørnstad et al. 1999). So, interpreting static and temporal diversity patterns requires explicit attention to spatial scale and correlation structure. Beyond interannual variability, long-term climatic regimes (e.g., mean temperature, precipitation, and seasonality) constrain species pools, life-history strategies, and dispersal capacities, thereby shaping baseline community composition and turnover potential across regions (Tonkin et al. 2017, Khaliq et al. 2024). Although such regimes provide the broader environmental template within which stochastic fluctuations operate, our focus here is on interannual variability and spatial synchrony as proximate drivers of temporal compositional change.

These contrasting dynamics are expected to influence temporal changes in spatial β-diversity (Tatsumi et al. 2021). Asynchronous, drift-like turnover can maintain or amplify spatial β-diversity over time, whereas synchronized environmental factors tends to homogenize communities across sites. Both processes can also increase local extinction risk when populations are small (Lande et al. 2003), and the spatial pattern of extinctions determines whether communities differentiate or homogenize through time (Olden et al. 2004). The balance between drift, environmental selection, and dispersal ultimately determines how local population fluctuations scale up to regional compositional change, even

though dispersal and spatial averaging may mitigate these effects (Arim et al. 2023, Suzuki and Economo 2024).

Disentangling these mechanisms in observational data is difficult because unmeasured or noisy environmental drivers can mimic demographic signals. Empirical studies therefore rely on indirect, pattern-based approaches rather than explicit variance partitioning, reflecting the limits of observational time series. For example, previous work has used community size (e.g., total number of individuals; Orrock & Watling, 2010) and area (Liu et al. 2018) as proxies for susceptibility to demographic noise, comparing observed patterns to null simulations, and applying dynamic models that partition demographic and environmental stochasticity (Cohen et al. 2013, Nakadai 2021, Knape et al. 2023). Thus, in observational studies community size is treated as a composite, indirect proxy for susceptibility to demographic variance, rather than as a direct measure of demographic stochasticity per se. For example, if smaller communities exhibit higher compositional variability or weaker environmental relationships, this suggests demographic noise plays a role, while acknowledging that temporal β-diversity may also reflect species-specific environmental responses, transient colonization–extinction dynamics, and observation error (Gilbert and Levine 2017, Siqueira et al. 2020). Recent research supported this strategy by showing that while the strength of environmental filtering increased with community size, spatial β-diversity in fish communities decreased (Jacobi and Siqueira 2023). However, large-scale empirical tests that simultaneously evaluate local and regional compositional variability across nested spatial extents and interpret these patterns against explicit stochastic baselines remain rare. This limitation hampers our ability to rigorously distinguish demographic scaling from environmentally structured spatial dynamics.

Considering this framing and the widespread population declines that potentially increase vulnerability to demographic noise (McCallum 2015, He et al. 2019, Almond et al.

2020), we investigated how the relative influence of demographic stochasticity and environmental variability on compositional dynamics (temporal β-diversity and temporal changes in spatial β-diversity) shifts across spatial scales. At the local scale, where population sizes are finite and demographic noise is expected to be strongest, we predicted that (1) abundance-based temporal β-diversity should increase as mean community size decreases, reflecting greater susceptibility to drift-like fluctuations. In contrast, at broader spatial scales, we predicted that (2) spatially synchronized environmental variation would better explain temporal changes in spatial β-diversity, consistent with environmental forcing increasingly shaping regional compositional dynamics once local demographic fluctuations are aggregated across sites. Also, because our response variables quantify inter-annual changes in composition, we emphasized environmental dimensions that vary among years and synchronize across sites, while treating longer-term climatic regimes as contextual constraints rather than direct drivers of temporal turnover.

To test these expectations, we first used simulations to validate whether β-diversity metrics reliably captured demographic variability under neutral-like dynamics that excluded environmental heterogeneity and niche differentiation, thereby establishing a demographic baseline for metric behaviour. We then analyzed 468 fish-community time series (1981–2019; 39 regions), modeling local and regional compositional variability against community size, environmental drivers, and species richness. By combining simulation and large-scale empirical analyses, we evaluated whether observed scaling relationships align with stochastic baseline expectations or instead indicate additional environmentally structured regional dynamics.

Material and methods

Data

149 We ran our empirical analyses using data from three databases. From the RivFishTIME
150 (Comte et al. 2021), we obtained time series count data of riverine fish around the globe.
151 TerraClimate (Abatzoglou et al. 2018) provided high-resolution monthly and WorldClim
152 (Fick and Hijmans 2017) provided annual mean and seasonality data for environmental
153 variables, from which we extracted time series data for precipitation, maximum air
154 temperature, and minimum air temperature (which is a good proxy for water temperature
155 (Stefan and Preud'homme 1993).

156 We defined a metacommunity as the set of sites within basin delineations
157 (HydroBASINS level 7) (Lehner and Grill 2013) and assigned a Strahler stream order for
158 each sampled site using information from the HydroRIVERS network (Lehner and Grill
159 2013). We then selected metacommunities that met the following criteria: (1) comprised at
160 least five communities in first to third-order streams, (2) were sampled at least four times in
161 different years, and (3) had at least five species. When dealing with metacommunity data
162 comprising multiple sampling events per year, we selected the sampling date with the highest
163 number of sampled sites to maximize the sample size. We selected these thresholds
164 pragmatically to balance spatial replication (minimum number of communities), temporal
165 replication (minimum number of years), and sufficient community complexity for reliable
166 estimation of β-diversity metrics. These steps resulted in 468 communities distributed within
167 39 metacommunities, sampled from 1981 to 2019, located in the Australasia (12), Nearctic
168 (12), and Palearctic (15) biogeographical realms (see Appendix S1: Figure S1). These
169 metacommunities were composed on average of 12 communities (standard deviation = 9)
170 sampled, on average, 11 times in the time-series (standard deviation = 5) with an average
171 temporal extent of 14 years (standard deviation = 5). All data selection and manipulation
172 were performed in R v. 4.2.1 (www.r-project.org) using the packages ncdf4 (Pierce 2023),
173 mapview (Appelhans et al. 2023) raster (Hijmans et al. 2023), sf (Pebesma 2018, Pebesma

and Bivand 2023), sp (Pebesma and Bivand 2005, Bivand et al. 2013), and tidyverse (Wickham et al. 2019).

Metrics of community size and species richness

We quantified local community size as the median number of individuals over time, representing the central tendency of population vulnerability to demographic stochasticity; that is, smaller values indicated communities where demographic stochasticity was more likely to occur. At the regional scale, we calculated metacommunity size as the median of these local medians over time. In addition to these measures of central tendency, we also included the temporal coefficient of variation (CV) in community size as a predictor of compositional variability at both local and regional scales.

Additionally, we calculated the proportion of species in the lowest abundance category (PL), which represents the share of relatively rare species in the regional species pool, following (Xiao et al. 2025). For each site we defined PL as the proportion of species whose mean abundance over the time series (for that specific site) fell in the lowest abundance bin of the observed species–abundance distribution, and we computed an analogous PL for each region. PL at the local scale was calculated by considering the whole set of samples within a community through time (the whole time series for each community) as the species pool. For regional PL, we calculated PL at the metacommunity level (the whole metacommunity was the species pool) for each time step and then used the median of these values for each metacommunity. For our regional models, we also included the temporal coefficient of variation (CV) of PL to account for fluctuations in the relative share of rare species through time. We included PL as an additional predictor at both local and regional scales because the share of relatively rare species may modulate susceptibility to demographic drift and to environment-driven losses, and thus influence temporal β-diversity.

To represent local species richness, we estimated the median asymptotic richness of each community over time. At the regional scale, we estimated gamma diversity as the median asymptotic richness of each metacommunity over time. Asymptotic richness was estimated with the iNEXT package (Hsieh et al. 2022), which combines extrapolation and interpolation techniques.

Environmental predictors of temporal variability in species composition

Environmental predictors of temporal variability in species composition included the coefficient of variation (CV) of maximum (CV tmax) and minimum (CV tmin) temperature and of precipitation (CV ppt). These metrics were measured by dividing the standard deviation of temperature and precipitation values at each site over time by the mean of these values.

We measured environmental synchrony within metacommunities by calculating the correlation of each environmental variable between communities over time (synchrony of maximum temperature = syn tmax, synchrony of minimum temperature = syn tmin, synchrony of precipitation = syn ppt). A high correlation or environmental synchrony would indicate that the environmental conditions being analyzed changed similarly across sites, while a low synchrony indicates that environmental conditions vary more independently across sites. Our focus on interannual variability and spatial synchrony reflects our interest in temporal drivers of compositional change, rather than in mean climatic conditions or seasonality per se.

Finally, we also investigated if sample size (number of samples collected) and time series length (temporal extent of sampling) at both community and metacommunity levels, and metacommunity spatial extent could counfound the estimated relationships. We measured the spatial extent of each metacommunity by calculating the mean Euclidean

distance between the central point of each metacommunity and its constituent communities. The mean distance between communities provides a measure of the overall spatial extent of the region encompassed by the metacommunity. We used the geosphere package (Hijmans 2022) to perform these calculations.

Metrics of temporal variability in species composition

A major challenge involved in relating community size to metrics of spatial and temporal variability in species composition is that they can be mathematically related to each other regardless of the underlying assembly process (Beck et al. 2013, Chase and Knight 2013, Barwell et al. 2015, Cao et al. 2021b). Thus, to select appropriate metrics of temporal variability that could be modeled against community size, we first simulated metacommunities without environmental heterogeneity and niche differentiation, such that species were ecologically equivalent and community dynamics were governed solely by stochastic birth–death processes and dispersal, according to the following steps.

Riverine networks were simulated using the mcbrnet R package (Terui and Pomeranz 2023). We first simulated random branching networks using the function brnet, which were then used in the mcsim function to simulate metacommunity dynamics. Since we were interested in simulating metacommunities without niche differentiation, we simulated species with similar niches along a spatially homogeneous environment by setting species to share identical niche optima (niche_optim = 0) and removing environmental heterogeneity (sd_env = 0; spatial_env_cor = FALSE). Carrying capacity was similar within communities in a given metacommunity but varied randomly among metacommunities (ranging from 50 to 150 individuals) and was specified at the patch level, such that all species within a community were regulated by a shared total carrying capacity. We manipulated random mortality intensity and carrying capacity to approximate metacommunity sizes observed in the

empirical datasets. We assigned the same dispersal probability to all species in each simulation but conducted multiple simulations with different probabilities (high: 1, intermediate: 0.5, low: 0.1) to assess their impact on the relationship between a metric of temporal variability and community size. Dispersal probability represented the likelihood that locally produced offspring emigrated to a connected patch within the branching network, with movement constrained by network connectivity.

Each simulation included 39 metacommunities, matching the empirical dataset. These metacommunities contained 5 to 30 communities and 5 to 48 species, reflecting the observed numbers in the empirical data. We ran each simulation for a total of 1000 time steps. After that, we selected species composition in ten time-steps (100, 200, 300, 400, 500, 600, 700, 800, 900, and 1000) as our temporal samples to measure the temporal variability at both local (within each community) and regional (among communities) scales using different metrics: (i) temporal variability in species composition at the local and regional scales, employing the metric proposed by Lamy *et al.*, (2021) and implemented in the ltmc package (Sokol and Lamy 2022) and (ii) temporal beta diversity, measured as the median of species rank changes (Avolio et al. 2019) within each community over time, using the RAC_change function in the codyn package (Hallett et al. 2016), and (iii) temporal variation in spatial turnover within metacommunities, via the RAC_difference function in the codyn package (Hallett et al. 2016). The median difference in species rank among communities within metacommunities was calculated at each time step.

Finally, we regressed all these metrics of temporal variability against median community size over time and compared the outcomes. Because these simulations excluded environmental heterogeneity and niche differentiation, any relationship between community size and compositional metrics arises solely from intrinsic stochastic demographic processes operating under neutral assumptions, without additional environmental forcing or sampling

effects (as full simulated community states were analysed without subsampling). This neutral baseline therefore allows us to assess whether observed size dependence in candidate β-diversity metrics reflects demographic scaling inherent to stochastic population dynamics or additional mathematical coupling with abundance distributions independent of demographic scaling. Metrics that show strong size dependence under these neutral conditions may conflate demographic scaling with statistical properties of abundance distributions, whereas metrics that remain insensitive to size provide a more conservative basis for interpreting empirical patterns.

Linear models

Modelling temporal β-diversity

The response variable selected to represent temporal variability in species composition, rank change (see results), represents values bounded between 0 and 1. To meet model assumptions of homoscedasticity and normality of residuals for Gaussian models, rank change was transformed using a logit transformation with a small offset (1e-6) to avoid zeros. Predictor variables were standardized (mean = 0, SD = 1) to improve model convergence and facilitate interpretation of effect sizes. We assessed multicollinearity among all predictors using variance inflation factors (VIF), and all values were below 2, indicating no cause for concern. We also tested for and found no significant correlation between rank change and two potential confounding variables, time series length and number of samples per time point. As we had no a priori hypotheses for these variables, they were excluded from the final models to aid interpretation and avoid overfitting.

We evaluated a series of increasingly complex linear models to explain temporal variability in local species composition (logit–transformed rank change). First, we fitted a beta regression including our standardized predictors: median community size, its temporal

coefficient of variation (CV), the proportion of species in the lowest abundance category (PL), estimated richness, and the CV of minimum temperature, maximum temperature, and precipitation. Next, we added a random intercept for metacommunity identity to account for non-independence among sites, and then introduced a dispersion submodel so that residual variance could vary as a function of community size, CV of community size, and PL. Likelihood-ratio tests and AIC comparisons showed that both the random effect and the heteroskedasticity component improved model fit (Appendix S1: Table S1).

Because our response is bounded between 0 and 1, we then refitted this full structure under both beta and Gaussian families. Although AIC favored the beta formulation, graphical and statistical diagnostics of residuals from the beta model (using DHARMa simulated-residual tests) revealed major issues with dispersion and quantile deviations. In contrast, the same diagnostics showed that the Gaussian location–scale model more closely met underlying assumptions, with a uniform QQ-plot and no dispersion issues. Furthermore, a check for out-of-bounds predictions from the Gaussian model found that none of the predictions fell outside the [0,1] interval. Based on these checks, we selected the Gaussian location–scale model for all subsequent inference.

To account for the possibility that long-term climatic regimes provide the ecological context within which inter-annual variability and demographic processes operate, we systematically incorporated additional climate variables into this base model. We sequentially added mean annual temperature, annual precipitation, temperature seasonality, precipitation seasonality, and temperature annual range, each time checking variance inflation factors (VIF) to avoid multicollinearity. Candidate models were compared using AIC, and the best-supported model included mean annual temperature and temperature seasonality alongside the original predictors, while retaining the random basin intercept and dispersion subformula (Appendix S1: Table S2).

Spatial autocorrelation in model residuals was initially strong (Moran's I = 0.192, $p < 0.001$). To address this, we incorporated spatial polynomials of latitude and longitude, including second-order terms and their interaction. This substantially reduced residual spatial autocorrelation (Moran's I = 0.045, p = 0.003) and improved model fit (ΔAIC = –26.1). We also tested nesting basins within freshwater ecoregions, but this additional random effect did not improve model fit (ΔAIC = +2.0) and was therefore not retained. The final model thus includes basin-level random intercepts, spatial polynomials, and the heteroskedastic dispersion subformula.

We estimated model explanatory power using marginal and conditional R^2 values derived from the location component of the Gaussian GLMM, which included fixed effects and a random intercept for metacommunity identity. These R^2 values quantify the proportion of variance explained by the fixed effects alone (marginal R^2) and by both fixed and random effects combined (conditional R^2), but do not account for variation explained by the dispersion (variance) model.

Modelling temporal changes in spatial β-diversity

To analyze temporal changes in spatial β-diversity, we followed a similar model-building and selection procedure as we did for temporal β-diversity. The response variable, the coefficient of variation in species ranks across sites within a metacommunity (CV_rank), is also a proportional measure bounded between 0 and 1. Consequently, it was logit-transformed with a small offset (1e-6) to avoid zeros, and all predictor variables were standardized (mean = 0, SD = 1). We again tested for correlations with time series length and number of samples per time point. Because we found none, we excluded these variables from subsequent models as they were not part of our core hypotheses.

We then assessed multicollinearity among our candidate predictors. Variance inflation factors (VIF) identified high collinearity among the temperature and precipitation synchrony metrics. We retained only synchrony in precipitation, which is most biologically relevant for our study systems, resulting in all VIF values below acceptable thresholds. Similarly, mean annual temperature, temperature seasonality, and temperature annual range exhibited high VIF values (>5) and were therefore excluded from the candidate set to avoid multicollinearity.

We then evaluated a series of models. First, we fitted a beta regression with a logit link including all standardized predictors. Unlike the model for temporal β-diversity, the addition of a dispersion submodel (allowing residual variance to vary as a function of metacommunity community size, median proportion of rare species, synchrony in precipitation, and regional CV of community size) did not improve model fit (LRT: $\chi^2 = 7.94$, df = 4, p = 0.094). We therefore proceeded with the simpler homoscedastic beta regression.

We compared this beta GLM to a Gaussian GLM with an identity link. In contrast to our model for temporal β-diversity, AIC favored the beta model (ΔAIC = 10.2; Appendix S1). Diagnostic checks using DHARMa revealed no issues with dispersion, uniformity, or outliers for the beta model, confirming that it met all necessary assumptions. A check for out-of-bounds predictions confirmed that none of the predictions fell outside the [0,1] interval.

We tested the inclusion of mean annual precipitation and precipitation seasonality as additional fixed effects in the beta regression framework. Neither variable improved model fit (ΔAIC = +2.55, p = 0.48), and both were non-significant predictors of spatial β-diversity variability. We also examined whether accounting for broad-scale spatial structure or ecoregion identity was necessary. A test for residual spatial autocorrelation was non-significant (Moran's I = –0.106, p = 0.39), and the addition of a random intercept for freshwater ecoregion did not improve model fit (ΔAIC = +2.00).

373 Based on these results, we selected the homoscedastic beta regression for all
374 subsequent inference. A full summary of the model selection procedure, including AIC
375 values for all compared models, is provided in Appendix S1: Table S1.
376 All model fitting was conducted in glmmTMB (Brooks et al. 2017), residuals were
377 checked with DHARMa (Hartig 2024), and p-values for fixed effects were obtained from
378 Type II Wald χ^2 tests in the car package (Fox and Weisberg 2019). All analyses were
379 conducted in R version 4.2.1 (R Core Team, 2022).
380
381 **Results**
382 **Metrics of temporal variability in simulated metacommunities**
383 Our simulations indicated that most metrics of temporal variability in species
384 composition had a relationship with community size. The LTMC metric (temporal turnover
385 within communities) exhibited a consistent negative relationship with community size at the
386 local scale and, at the regional scale, showed a negative relationship in some simulations,
387 whereas in others no such pattern was observed (see Appendix S1: Table S2). However,
388 when a relationship was present at the regional scale, it exhibited high explanatory power.
389 The species rank difference metric was positively related to community size in most
390 simulations at the regional scale; however, the explanatory power of the models (R^2) was
391 consistently low across all simulation scenarios (mean $R^2 = 0.03$; see Appendix S1: Table
392 S2). The species rank change metric (temporal variability in rank abundance curves) was the
393 only metric that was consistently not related to community size at the local scale (see
394 Appendix S1: Table S2).
395 Thus, because the rank-abundance metrics showed no consistent size dependence
396 under neutral-like dynamics, we used them to analyze the empirical data. More specifically,
397 to represent temporal variability in species composition for each community (temporal β-

diversity within communities), we used the species-rank change metric. To represent temporal changes in spatial β-diversity within metacommunities, we used the coefficient of variation of rank differences across years.

Relationships in the empirical dataset

Temporal β-diversity

The final Gaussian location-scale mixed model (family: Gaussian, link: identity) explained 29.8% of the variance in temporal β-diversity (conditional $R^2 = 0.298$; marginal $R^2 = 0.294$). Temporal β-diversity was influenced by both community properties and climatic regimes (Table 1).

In the conditional (mean) component of the model, median community size was negatively related to compositional variability (β = -0.004, SE = 0.002; Wald $\chi^2 = 5.15$, df = 1, p = 0.0023; Figure 1a), while temporal variability in community size (CV) was positively related (β = 0.012, SE = 0.002; Wald $\chi^2 = 25.25$, df = 1, p = 5.02e-07; Figure 1b). Local species richness was also positively related to temporal β-diversity (β = 0.014, SE = 0.003; Wald $\chi^2 = 18.40$, df = 1, p = 1.79e-05; Figure 1c). The proportion of species in the lowest abundance category (PL) was not a main predictor of temporal β-diversity. Both mean annual temperature (β = 0.045, SE = 0.018; Wald $\chi^2 = 6.19$, p = 0.013) and temperature seasonality (β = 0.070, SE = 0.009; Wald $\chi^2 = 52.80$, p = 3.69e-13) were strong positive predictors, with temperature seasonality showing the largest effect among all covariates (Table 1).

The dispersion component of the model revealed that residual variance declined with increasing community size (β = -0.665, SE = 0.079; z = -8.45, p = 2e-16), temporal variability in community size (β = -0.245, SE = 0.070; z = -3.51, p = 0.0004), and the proportion of species in the lowest abundance category (β = -0.334, SE = 0.063; z = -5.33, p = 1.19e-07).

Temporal changes in spatial β-diversity

The beta regression model (family: beta, link: logit) explained 31% of the variance in temporal variability of spatial β-diversity (Ferrari's $R^2 = 0.311$). Variability was primarily influenced by environmental synchrony and only marginally by community properties (Table 2). Spatial synchrony in precipitation was negatively related to variability in spatial β-diversity ($\beta = -0.153$, SE = 0.073; Wald $\chi^2 = 4.42$, df = 1, $p = 0.036$), indicating that metacommunities in regions with more synchronized precipitation conditions across sites exhibited more stable spatial structure over time.

The coefficient of variation in community size showed a positive, marginal relationship with temporal variability in spatial β-diversity ($\beta = 0.138$, SE = 0.076; Wald $\chi^2 = 3.29$, df = 1, $p = 0.069$). Community size, gamma diversity, the proportion of rare species, its variability, and mean distance among sites had no effect on temporal variability in spatial β-diversity (Table 2).

Discussion

Our research indicates that demographic stochasticity scales up to structure temporal β-diversity, with environmental factors becoming progressively dominant at broader spatial scales. At the local scale, temporal β-diversity was higher in communities with smaller populations, greater fluctuations in total community abundance and higher species richness. Climatic regime variables, particularly temperature seasonality, were positively associated with local temporal β-diversity, indicating that inter-annual compositional dynamics unfold within broader environmental contexts (Qian et al. 2009, Keil et al. 2012). At the regional scale, temporal variability in spatial β-diversity was primarily associated with the spatial synchrony of precipitation, with more synchronized environments exhibiting lower regional

448 compositional variability. Together, these findings indicate that the interplay between
449 demographic stochasticity and environmental selection determines the degree and
450 predictability of compositional change across spatial scales, reflecting a mechanistic rather
451 than statistical transition in dominant drivers.

452 Our finding that temporal β-diversity is higher in small and more variable (in size)
453 communities highlights how demographic stochasticity can scale up to shape community
454 dynamics. We emphasize that community size functions here as an indirect proxy for
455 susceptibility to demographic variance, integrating species with different abundances, life
456 histories, and sensitivities to environmental variation, and potentially also observation error.
457 But there is no doubt that when mean abundance is low, each birth or death event represents a
458 larger proportional change in population size, amplifying random fluctuations that
459 accumulate through time and increasing the probability of local extinction (Lande, 1993).
460 High temporal variance in community size may further weaken deterministic fitness
461 differences, promoting rank reshuffling (Orrock and Watling 2010, Gilbert and Levine 2017,
462 Legault et al. 2019) and extinction-recolonization dynamics, increasing compositional
463 unpredictability (Leibold and Chase 2018, Tabi et al. 2024). The dispersion component of our
464 model reinforces this interpretation, as residual variance declined strongly with increasing
465 mean community size, consistent with the inverse scaling of demographic stochasticity with
466 population size.

467 Beyond demographic influences, the climatic context serves as a macroecological
468 template for communities. Temperature seasonality was the strongest climatic correlate of
469 temporal β-diversity, with higher intra-annual thermal variability associated with greater
470 inter-annual compositional change; mean annual temperature also showed a positive
471 relationship. Riverine communities embedded in more seasonal environments may
472 experience stronger life-history filtering (Hernández-Carrasco et al. 2025). Conversely, in

warmer climates, communities may be more subject to stochastic assembly processes, as higher temperatures accelerate metabolic rates and generation times, leading to smaller population sizes and greater demographic stochasticity (Saito et al. 2021a, 2021b), thereby amplifying intra- and inter-annual compositional variability (Coffman and de la Rosa 1998, Siqueira et al. 2008, Hernández-Carrasco et al. 2025). Thus, in systems where seasonal filtering produces communities of species with narrow environmental tolerances, inter-annual climatic deviations may trigger disproportionately large compositional responses, potentially amplifying the intrinsic variability already associated with warmer temperatures. Species richness was also positively correlated with temporal β-diversity, consistent with more diverse communities having a wider pool of colonists and alternative trait combinations that increase the number of potential community states (Leibold and Chase 2018, Saito et al. 2021b, Arim et al. 2023). However, because rank_change captures relative reordering across the full species pool, its sensitivity varies with richness (Hallett et al. 2016). In species-poor communities, a single species replacement generates larger rank shifts than equivalent turnover in richer communities. The positive richness–β-diversity relationship may therefore partly reflect differences in metric sensitivity across the restricted, temperate-biased diversity gradient in our dataset (Cao et al. 2021a, Hernández-Carrasco et al. 2026), rather than solely greater ecological dynamism in species-rich systems.

Rather than explicitly partitioning demographic and environmental variance as in parametric population-dynamic frameworks (e.g., Sæther et al. 2013), we infer their relative influence using scale-explicit compositional metrics. Our simulation baseline supports this inference. Under purely stochastic dynamics without environmental structure, the rank_change metric showed no systematic relationship with community size across scales. This indicates that the observed scaling pattern is unlikely to arise from metric artefacts alone and is consistent with a contribution of demographic stochasticity to local compositional

variability. Because rank shifts are nonlinearly related to abundance fluctuations, however, small changes near rank boundaries can generate disproportionate changes in ordering. The rank_change metric therefore captures relative compositional reorganization rather than direct estimates of demographic variance, and abundance-based parametric models would complement this approach by explicitly decomposing these components. Crucially, the empirical patterns diverge from the simulated stochastic baseline in an ecologically informative way. Instead of the scale-invariant relationship predicted by the simulations, we observed a strong negative relationship locally and little to none regionally, which is consistent with local demographic susceptibility but regional environmental forcing.

Shifting from local to regional scale, a fundamentally different mechanism emerged. In river networks, spatially synchronized precipitation can induce correlated hydrological responses across catchments – a Moran-type effect (Ranta et al. 1997, Liebhold et al. 2004) extended to community composition – reducing opportunities for asynchronous species turnover and limiting spatial reorganization of communities through time. Consistent with this, we found a negative relationship between precipitation synchrony and temporal variability in spatial β-diversity. When environmental forcing is synchronized across sites, compensatory turnover is reduced, dampening regional compositional variability (Lamy et al. 2021). Unlike its strong local influence, the absence of a community-size effect at the regional scale is consistent with stochastic fluctuations being attenuated through spatial aggregation at regional scales rather than disappearing (Barbosa et al. 2025). The influence of precipitation synchrony is likely further mediated by dendritic network architecture. Because river networks are organized dendritically, hydrological pulses are integrated and propagated more extensively through well-connected mainstems than through isolated headwater streams (Campbell Grant et al. 2007), a process that amplifies spatial synchrony in both environmental conditions and community composition across the network (Ruhi et al. 2018).

Also, in dendritic networks, the dispersal of aquatic organisms can be mostly restricted to branching, directional pathways (Fagan 2002), creating a system where network position dictates connectivity (Siqueira et al. 2014, Terui et al. 2018). Explicitly incorporating network position into future analyses would allow a more mechanistic decomposition of environmental and dispersal-mediated components of temporal variations in spatial β-diversity. Although landscape features such as vegetation cover may further mediate hydrological, thermal, and compositional responses (Dala-Corte et al. 2020, Schneck et al. 2022, Collyer et al. 2023), resolving those interactions would require temporally explicit land-use data beyond the scope of this analysis.

Several caveats warrant consideration. First, community size is an indirect proxy for demographic susceptibility and does not measure per-capita demographic variance directly. Second, fish counts may be affected by imperfect detection that varies with abundance or habitat. Third, our environmental predictors are annual summaries (TerraClimate) and may miss ecologically important extremes or intra-annual hydrological dynamics (e.g., floods, droughts) that drive turnover in riverine systems. Fourth, requiring ≥4 temporal replicates produced a dataset strongly biased toward temperate regions, which constrains not only sample coverage but the interpretation of our climatic findings. The relationships involving temperature seasonality and mean annual temperature should therefore be understood as applying primarily to more seasonal riverine systems. Ecological processes structuring β-diversity differ across latitudinal gradients, and tropical systems, which are often characterized by distinct hydrological dynamics and higher diversity (Phillips et al. 2017, Shumilova et al. 2019), may exhibit markedly different climate–composition relationships. Expanding long-term monitoring in tropical regions is essential to evaluate generality.

Understanding these scale-dependent processes is essential in a time of widespread population declines (McCallum 2015, Leuenberger et al. 2025). Because demographic

548 stochasticity shapes population dynamics (Otto and Whitlock 1997, Whitlock 2004, Willi et
549 al. 2006), its effects scale up to communities. We identify a shift from demographic to
550 environmental forcing with increasing scale. At the local scale, demographic stochasticity
551 and climatic regime jointly structure compositional variability, whereas at the regional scale,
552 environmental factors predominate. By linking spatial scale to demographic and
553 environmental control, our study integrates population and community theory (Lande 1993,
554 Vindenes and Engen 2017, Leibold and Chase 2018) and provides a framework for
555 interpreting temporal β-diversity under environmental change. Future work combining long-
556 term standardized time series with parametric community models could directly estimate
557 demographic and environmental variance components, complementing the comparative,
558 scale-explicit approach adopted here.
559
560 **Acknowledgments:** We thank Holly Harris for commenting on previous versions of this
561 manuscript. We also thank the anonymous reviewers for their comments, which prompted a
562 thorough revision of the manuscript. The final version reflects, in part, revisions beyond the
563 scope of the original arguments, as shaped by the review process. We thank the Coordenação
564 de Aperfeiçoamento de Pessoal de Nível Superior - Brasil (CAPES) - Funding Code 001 for
565 providing a PhD scholarship to CMJ. TS is supported by funding from the Centre for
566 Research on Biodiversity Dynamics and Climate Change (FAPESP #2021/10639-5) and by a
567 Productivity Grant (Conselho Nacional de Desenvolvimento Científico e Tecnológico, CNPq
568 # 301319/2025-1). No fieldwork was conducted for this study, and therefore no permits or
569 permissions were required.

References

Abatzoglou, J. T., S. Z. Dobrowski, S. A. Parks, and K. C. Hegewisch. 2018. TerraClimate, a high-resolution global dataset of monthly climate and climatic water balance from 1958–2015. Scientific Data 5:170191.

Almond, R. E. A., M. Grooten, and T. Petersen. 2020. Bending the curve of biodiversity loss. WWF, Gland.

Appelhans, T., F. Detsch, C. Reudenbach, S. Woellauer, S. Forteva, T. Nauss, E. Pebesma, K. Russell, M. Sumner, J. Darley, P. Roudier, P. Schratz, E. I. Marburg, and L. Busetto. 2023, October 13. mapview: Interactive Viewing of Spatial Data in R.

Arim, M., V. Pinelli, L. Rodríguez-Tricot, E. Ortiz, M. Illarze, C. Fagúndez-Pachón, and A. I. Borthagaray. 2023. Chance and necessity in the assembly of plant communities: Stochasticity increases with size, isolation and diversity of temporary ponds. Journal of Ecology 111:1641–1655.

Avolio, M. L., I. T. Carroll, S. L. Collins, G. R. Houseman, L. M. Hallett, F. Isbell, S. E. Koerner, K. J. Komatsu, M. D. Smith, and K. R. Wilcox. 2019. A comprehensive approach to analyzing community dynamics using rank abundance curves. Ecosphere 10:e02881.

Barbosa, G. P., C. B. Vieira, A. Carolina Dos Santos, N. Lara, E. Mateus-Barros, J. L. Portinho, H. Sarmento, G. Perbiche-Neves, B. Veloso, C. Montagner, L. Schiesari, V. S. Saito, and T. Siqueira. 2025. Agrochemical effects on plankton temporal variability are buffered at larger spatial scales. Oikos 2025:e11436.

Barwell, L. J., N. J. B. Isaac, and W. E. Kunin. 2015. Measuring β-diversity with species abundance data. The Journal of Animal Ecology 84:1112–1122.

Beck, J., J. D. Holloway, and W. Schwanghart. 2013. Undersampling and the measurement of beta diversity. Methods in Ecology and Evolution 4:370–382.

Bivand, R., E. Pebesma, and V. Gomez-Rubio. 2013. Applied spatial data analysis with R, Second edition.

596 Bjørnstad, O. N., R. A. Ims, and X. Lambin. 1999. Spatial population dynamics: analyzing patterns
597 and processes of population synchrony. Trends in Ecology & Evolution 14:427–432.
598 Brooks, M. E., K. Kristensen, K. J. van Benthem, A. Magnusson, C. W. Berg, A. Nielsen, H. J. Skaug,
599 M. Mächler, and B. M. Bolker. 2017. glmmTMB Balances Speed and Flexibility Among
600 Packages for Zero-inflated Generalized Linear Mixed Modeling. The R Journal 9:378–400.
601 Campbell Grant, E. H., W. H. Lowe, and W. F. Fagan. 2007. Living in the branches: population
602 dynamics and ecological processes in dendritic networks. Ecology Letters 10:165–175.
603 Cao, K., R. Condit, X. Mi, L. Chen, H. Ren, W. Xu, D. F. R. P. Burslem, C. Cai, M. Cao, L.-W.
604 Chang, C. Chu, F. Cui, H. Du, S. Ediriweera, C. S. V. Gunatilleke, I. U. A. N. Gunatilleke, Z.
605 Hao, G. Jin, J. Li, B. Li, Y. Li, Y. Liu, H. Ni, M. J. O'Brien, X. Qiao, G. Shen, S. Tian, X.
606 Wang, H. Xu, Y. Xu, L. Yang, S. L. Yap, J. Lian, W. Ye, M. Yu, S.-H. Su, C.-H. Chang-Yang,
607 Y. Guo, X. Li, F. Zeng, D. Zhu, L. Zhu, I.-F. Sun, K. Ma, and J.-C. Svenning. 2021a. Species
608 packing and the latitudinal gradient in beta-diversity. Proceedings of the Royal Society B:
609 Biological Sciences 288:20203045.
610 Cao, K., J.-C. Svenning, C. Yan, J. Zhang, X. Mi, and K. Ma. 2021b. Undersampling correction
611 methods to control γ-dependence for comparing β-diversity between regions. Ecology
612 102:e03448.
613 Chase, J. M., and T. M. Knight. 2013. Scale-dependent effect sizes of ecological drivers on
614 biodiversity: why standardised sampling is not enough. Ecology Letters 16:17–26.
615 Coffman, W. P., and C. L. de la Rosa. 1998. Taxonomic Composition and Temporal Organization of
616 Tropical and Temperate Species Assemblages of Lotic Chironomidae. Journal of the Kansas
617 Entomological Society 71:388–406.
618 Cohen, J. E., M. Xu, and W. S. F. Schuster. 2013. Stochastic multiplicative population growth predicts
619 and interprets Taylor's power law of fluctuation scaling. Proceedings of the Royal Society B:
620 Biological Sciences 280:20122955.
621 Collyer, G., D. M. Perkins, D. K. Petsch, T. Siqueira, and V. Saito. 2023. Land-use intensification
622 systematically alters the size structure of aquatic communities in the Neotropics. Global
623 Change Biology 29:4094–4106.

624 Comte, L., J. Carvajal-Quintero, P. A. Tedesco, X. Giam, U. Brose, T. Erős, A. F. Filipe, M. Fortin, K.
625 Irving, C. Jacquet, S. Larsen, S. Sharma, A. Ruhi, F. G. Becker, L. Casatti, G. Castaldelli, R.
626 B. Dala-Corte, S. R. Davenport, N. R. Franssen, E. García-Berthou, A. Gavioli, K. B. Gido,
627 L. Jimenez-Segura, R. P. Leitão, B. McLarney, J. Meador, M. Milardi, D. B. Moffatt, T. V. T.
628 Occhi, P. S. Pompeu, D. L. Propst, M. Pyron, G. N. Salvador, J. A. Stefferud, T. Sutela, C.
629 Taylor, A. Terui, H. Urabe, T. Vehanen, J. R. S. Vitule, J. O. Zeni, and J. D. Olden. 2021.
630 RivFishTIME: A global database of fish time-series to study global change ecology in
631 riverine systems. Global Ecology and Biogeography 30:38–50.
632 Dala-Corte, R. B., A. S. Melo, T. Siqueira, L. M. Bini, R. T. Martins, A. M. Cunico, A. M. Pes, A. L.
633 B. Magalhães, B. S. Godoy, C. G. Leal, C. S. Monteiro-Júnior, C. Stenert, D. M. P. Castro, D.
634 R. Macedo, D. P. Lima-Junior, É. A. Gubiani, F. C. Massariol, F. B. Teresa, F. G. Becker, F. N.
635 Souza, F. Valente-Neto, F. L. Souza, F. F. Salles, G. L. Brejão, J. G. Brito, J. R. S. Vitule, J.
636 Simião-Ferreira, K. Dias-Silva, L. Albuquerque, L. Juen, L. Maltchik, L. Casatti, L. Montag,
637 M. E. Rodrigues, M. Callisto, M. A. M. Nogueira, M. R. Santos, N. Hamada, P. A. Z.
638 Pamplin, P. S. Pompeu, R. P. Leitão, R. Ruaro, R. Mariano, S. R. M. Couceiro, V. Abilhoa, V.
639 C. Oliveira, Y. Shimano, Y. Moretto, Y. R. Súarez, and F. de O. Roque. 2020. Thresholds of
640 freshwater biodiversity in response to riparian vegetation loss in the Neotropical region.
641 Journal of Applied Ecology 57:1391–1402.
642 Doak, D. F., D. Bigger, E. K. Harding, M. A. Marvier, R. E. O'Malley, and D. Thomson. 1998. The
643 Statistical Inevitability of Stability-Diversity Relationships in Community Ecology. The
644 American Naturalist 151:264–276.
645 Dornelas, M., J. M. Chase, N. J. Gotelli, A. E. Magurran, B. J. McGill, L. H. Antão, S. A. Blowes, G.
646 N. Daskalova, B. Leung, I. S. Martins, F. Moyes, I. H. Myers-Smith, C. D. Thomas, and M.
647 Vellend. 2023. Looking back on biodiversity change: lessons for the road ahead.
648 Philosophical Transactions of the Royal Society B: Biological Sciences 378:20220199.
649 Fagan, W. F. 2002. Connectivity, Fragmentation, and Extinction Risk in Dendritic Metapopulations.
650 Ecology 83:3243–3249.

651 Fick, S. E., and R. J. Hijmans. 2017. WorldClim 2: new 1-km spatial resolution climate surfaces for
652 global land areas. International Journal of Climatology 37:4302–4315.
653 Fox, J., and S. Weisberg. 2019. An {R} Companion to Applied Regression, Third Edition. Thousand
654 Oaks CA: Sage.
655 Gilbert, B., and J. M. Levine. 2017. Ecological drift and the distribution of species diversity.
656 Proceedings of the Royal Society B: Biological Sciences 284:20170507.
657 Gonzalez, A., and M. Loreau. 2009. The Causes and Consequences of Compensatory Dynamics in
658 Ecological Communities. Annual Review of Ecology, Evolution, and Systematics 40:393–
659 414.
660 Hallett, L. M., S. K. Jones, A. A. M. MacDonald, M. B. Jones, D. F. B. Flynn, J. Ripplinger, P.
661 Slaughter, C. Gries, and S. L. Collins. 2016. CODYN: An R package of community dynamics
662 metrics. Methods in Ecology and Evolution 7:1146–1151.
663 Hammond, M., M. Loreau, C. de Mazancourt, and J. Kolasa. 2020. Disentangling local,
664 metapopulation, and cross-community sources of stabilization and asynchrony in
665 metacommunities. Ecosphere 11:e03078.
666 Hartig, F. 2024. DHARMa: Residual Diagnostics for Hierarchical (Multi-Level / Mixed) Regression
667 Models.
668 He, F., C. Zarfl, V. Bremerich, J. N. W. David, Z. Hogan, G. Kalinkat, K. Tockner, and S. C. Jähnig.
669 2019. The global decline of freshwater megafauna. Global Change Biology 25:3883–3892.
670 Hernández-Carrasco, D., A. J. Gillis, H. R. Lai, T. Siqueira, and J. D. Tonkin. 2026. Accounting for
671 the Influence of Community Turnover Along Environmental Gradients on Compositional
672 Uniqueness. Ecology Letters 29:e70338.
673 Hernández-Carrasco, D., J. M. Tylianakis, D. A. Lytle, and J. D. Tonkin. 2025. Ecological and
674 evolutionary consequences of changing seasonality. Science 388:eads4880.
675 Hijmans, R. 2022. _geosphere: spherical trigonometry_.
676 Hijmans, R. J., J. van Etten, M. Sumner, J. Cheng, D. Baston, A. Bevan, R. Bivand, L. Busetto, M.
677 Canty, B. Fasoli, D. Forrest, A. Ghosh, D. Golicher, J. Gray, J. A. Greenberg, P. Hiemstra, K.
678 Hingee, A. Ilich, I. for M. A. Geosciences, C. Karney, M. Mattiuzzi, S. Mosher, B. Naimi, J.

679 Nowosad, E. Pebesma, O. P. Lamigueiro, E. B. Racine, B. Rowlingson, A. Shortridge, B.
680 Venables, and R. Wueest. 2023, October 14. raster: Geographic Data Analysis and Modeling.
681 Hsieh, T., K. Ma, and A. Chao. 2022. iNEXT: iNterpolation and EXTrapolation for species diversity.
682 Jacobi, C. M., and T. Siqueira. 2023. High compositional dissimilarity among small communities is
683 decoupled from environmental variation. Oikos 2023:e09802.
684 Kéfi, S., V. Domínguez-García, I. Donohue, C. Fontaine, E. Thébault, and V. Dakos. 2019. Advancing
685 our understanding of ecological stability. Ecology Letters 22:1349–1356.
686 Keil, P., O. Schweiger, I. Kühn, W. E. Kunin, M. Kuussaari, J. Settele, K. Henle, L. Brotons, G. Pe'er,
687 S. Lengyel, A. Moustakas, H. Steinicke, and D. Storch. 2012. Patterns of beta diversity in
688 Europe: the role of climate, land cover and distance across scales. Journal of Biogeography
689 39:1473–1486.
690 Khaliq, I., C. Rixen, F. Zellweger, C. H. Graham, M. M. Gossner, I. R. McFadden, L. Antão, J.
691 Brodersen, S. Ghosh, F. Pomati, O. Seehausen, T. Roth, T. Sattler, S. R. Supp, M. Riaz, N. E.
692 Zimmermann, B. Matthews, and A. Narwani. 2024. Warming underpins community turnover
693 in temperate freshwater and terrestrial communities. Nature Communications 15:1921.
694 Knape, J., M. Paquet, D. Arlt, I. Kačergytė, and T. Pärt. 2023. Partitioning variance in population
695 growth for models with environmental and demographic stochasticity. Journal of Animal
696 Ecology 92:1979–1991.
697 Lamy, T., N. I. Wisnoski, R. Andrade, M. C. N. Castorani, A. Compagnoni, N. Lany, L. Marazzi, S.
698 Record, C. M. Swan, J. D. Tonkin, N. Voelker, S. Wang, P. L. Zarnetske, and E. R. Sokol.
699 2021. The dual nature of metacommunity variability. Oikos 130:2078–2092.
700 Lande, R. 1993. Risks of Population Extinction from Demographic and Environmental Stochasticity
701 and Random Catastrophes. The American Naturalist 142:911–927.
702 Lande, R., S. Engen, and B.-E. Sæther. 2003. Stochastic Population Dynamics in Ecology and
703 Conservation. Oxford University Press.
704 Legault, G., J. W. Fox, and B. A. Melbourne. 2019. Demographic stochasticity alters expected
705 outcomes in experimental and simulated non-neutral communities. Oikos 128:1704–1715.

706 Lehner, B., and G. Grill. 2013. Global river hydrography and network routing: baseline data and new
707 approaches to study the world's large river systems. Hydrological Processes 27:2171–2186.
708 Leibold, M. A., and J. M. Chase. 2018. Metacommunity Ecology, Volume 59. Princeton University
709 Press, Princeton, NJ.
710 Leuenberger, W., J. W. Doser, M. W. Belitz, L. Ries, N. M. Haddad, W. E. Thogmartin, and E. F.
711 Zipkin. 2025. Three decades of declines restructure butterfly communities in the Midwestern
712 United States. Proceedings of the National Academy of Sciences 122:e2501340122.
713 Liebhold, A., W. D. Koenig, and O. N. Bjørnstad. 2004. Spatial Synchrony in Population Dynamics*.
714 Annual Review of Ecology, Evolution, and Systematics 35:467–490.
715 Liu, J., M. Vellend, Z. Wang, and M. Yu. 2018. High beta diversity among small islands is due to
716 environmental heterogeneity rather than ecological drift. Journal of Biogeography 45:2252–
717 2261.
718 Magurran, A. E., M. Dornelas, F. Moyes, and P. A. Henderson. 2019. Temporal β diversity—A
719 macroecological perspective. Global Ecology and Biogeography 28:1949–1960.
720 McCallum, M. L. 2015. Vertebrate biodiversity losses point to a sixth mass extinction. Biodiversity
721 and Conservation 24:2497–2519.
722 McCann, K. S., J. B. Rasmussen, and J. Umbanhowar. 2005. The dynamics of spatially coupled food
723 webs. Ecology Letters 8:513–523.
724 Melbourne, B. A., and A. Hastings. 2008. Extinction risk depends strongly on factors contributing to
725 stochasticity. Nature 454:100–103.
726 Nakadai, R. 2021. Individual-based multiple-unit dissimilarity: novel indices and null model for
727 assessing temporal variability in community composition. Oecologia 197:353–364.
728 Olden, J. D., N. L. Poff, M. R. Douglas, M. E. Douglas, and K. D. Fausch. 2004. Ecological and
729 evolutionary consequences of biotic homogenization. Trends in Ecology & Evolution 19:18–
730 24.
731 Orrock, J. L., and J. I. Watling. 2010. Local community size mediates ecological drift and competition
732 in metacommunities. Proceedings of the Royal Society B: Biological Sciences 277:2185–
733 2191.

Otto, S. P., and M. C. Whitlock. 1997. The Probability of Fixation in Populations of Changing Size. Genetics 146:723–733.

Pebesma, E. 2018. Simple Features for R: Standardized support for spatial vector data. The R Journal.

Pebesma, E., and R. Bivand. 2005. Classes and methods for spatial data in R. R News.

Pebesma, E., and R. Bivand. 2023. Spatial data science: with applications in R (1st ed.).

Phillips, H. R. P., T. Newbold, and A. Purvis. 2017. Land-use effects on local biodiversity in tropical forests vary between continents. Biodiversity and Conservation 26:2251–2270.

Pierce, D. 2023. ncdf4: Interface to Unidata netCDF (Version 4 or Earlier) Format Data Files_.

Qian, H., C. Badgley, and D. L. Fox. 2009. The latitudinal gradient of beta diversity in relation to climate and topography for mammals in North America. Global Ecology and Biogeography 18:111–122.

Ranta, E., V. Kaitala, J. Lindstr□m, and E. Helle. 1997. The Moran Effect and Synchrony in Population Dynamics. Oikos 78:136–142.

Reed, D. H., and G. R. Hobbs. 2004. The relationship between population size and temporal variability in population size. Animal Conservation 7:1–8.

Rezende, F., P. A. P. Antiqueira, O. L. Petchey, L. F. M. Velho, L. C. Rodrigues, and G. Q. Romero. 2021. Trophic downgrading decreases species asynchrony and community stability regardless of climate warming. Ecology Letters 24:2660–2673.

Ruhi, A., M. L. Messager, and J. D. Olden. 2018. Tracking the pulse of the Earth's fresh waters. Nature Sustainability 1:198–203.

Saito, V. S., D. M. Perkins, and P. Kratina. 2021a. A Metabolic Perspective of Stochastic Community Assembly. Trends in Ecology & Evolution 36:280–283.

Saito, V. S., N. E. Stoppa, E. M. Shimabukuro, M. Cañedo-Argüelles, N. Bonada, and T. Siqueira. 2021b. Stochastic colonisation dynamics can be a major driver of temporal β diversity in Atlantic Forest coastal stream communities. Freshwater Biology 66:1560–1570.

Schneck, F., L. M. Bini, A. S. Melo, D. K. Petsch, V. S. Saito, S. Wengrat, and T. Siqueira. 2022. Catchment scale deforestation increases the uniqueness of subtropical stream communities. Oecologia 199:671–683.

762 Shimadzu, H., M. Dornelas, and A. E. Magurran. 2015. Measuring temporal turnover in ecological
763 communities. Methods in Ecology and Evolution 6:1384–1394.
764 Shumilova, O., D. Zak, T. Datry, D. von Schiller, R. Corti, A. Foulquier, B. Obrador, K. Tockner, D.
765 C. Allan, F. Altermatt, M. I. Arce, S. Arnon, D. Banas, A. Banegas-Medina, E. Beller, M. L.
766 Blanchette, J. F. Blanco-Libreros, J. Blessing, I. G. Boëchat, K. Boersma, M. T. Bogan, N.
767 Bonada, N. R. Bond, K. Brintrup, A. Bruder, R. Burrows, T. Cancellario, S. M. Carlson, S.
768 Cauvy-Fraunié, N. Cid, M. Danger, B. de Freitas Terra, A. M. D. Girolamo, R. del Campo, F.
769 Dyer, A. Elosegi, E. Faye, C. Febria, R. Figueroa, B. Four, M. O. Gessner, P. Gnohossou, R.
770 G. Cerezo, L. Gomez-Gener, M. A. S. Graça, S. Guareschi, B. Gücker, J. L. Hwan, S.
771 Kubheka, S. D. Langhans, C. Leigh, C. J. Little, S. Lorenz, J. Marshall, A. McIntosh, C.
772 Mendoza-Lera, E. I. Meyer, M. Miliša, M. C. Mlambo, M. Moleón, P. Negus, D. Niyogi, A.
773 Papatheodoulou, I. Pardo, P. Paril, V. Pešić, P. Rodriguez-Lozano, R. J. Rolls, M. M. Sanchez-
774 Montoya, A. Savić, A. Steward, R. Stubbington, A. Taleb, R. V. Vorste, N. Waltham, A.
775 Zoppini, and C. Zarfl. 2019. Simulating rewetting events in intermittent rivers and ephemeral
776 streams: A global analysis of leached nutrients and organic matter. Global Change Biology
777 25:1591–1611.
778 Siqueira, T., L. D. Durães, and F. de O. Roque. 2014. Predictive Modelling of Insect
779 Metacommunities in Biomonitoring of Aquatic Networks. Pages 109–126 *in* C. P. Ferreira
780 and W. A. C. Godoy, editors. Ecological Modelling Applied to Entomology.
781 Siqueira, T., C. P. Hawkins, J. D. Olden, J. Tonkin, L. Comte, V. S. Saito, T. L. Anderson, G. P.
782 Barbosa, N. Bonada, C. C. Bonecker, M. Cañedo-Argüelles, T. Datry, M. B. Flinn, P. Fortuño,
783 G. A. Gerrish, P. Haase, M. J. Hill, J. M. Hood, K. Huttunen, M. J. Jeffries, T. Muotka, D. R.
784 O'Donnell, R. Paavola, P. Paril, M. J. Paterson, C. J. Patrick, G. Perbiche-Neves, L. C.
785 Rodrigues, S. C. Schneider, M. Straka, and A. Ruhi. 2024. Understanding temporal variability
786 across trophic levels and spatial scales in freshwater ecosystems. Ecology 105:e4219.
787 Siqueira, T., F. O. Roque, and S. Trivinho-Strixino. 2008. Phenological patterns of neotropical lotic
788 chironomids: Is emergence constrained by environmental factors? Austral Ecology 33:902–
789 910.

790 Siqueira, T., V. S. Saito, L. M. Bini, A. S. Melo, D. K. Petsch, V. L. Landeiro, K. T. Tolonen, J.
791 Jyrkänkallio-Mikkola, J. Soininen, and J. Heino. 2020. Community size can affect the signals
792 of ecological drift and niche selection on biodiversity. Ecology 101:e03014.
793 Sokol, E., and T. Lamy. 2022. _ltmc: Long-term metacommunity analysis_.
794 Stefan, H. G., and E. B. Preud'homme. 1993. Stream Temperature Estimation from Air Temperature1.
795 JAWRA Journal of the American Water Resources Association 29:27–45.
796 Steiner, C. F., R. D. Stockwell, V. Kalaimani, and Z. Aqel. 2013. Population synchrony and stability in
797 environmentally forced metacommunities. Oikos 122:1195–1206.
798 Suzuki, Y., and E. P. Economo. 2024. The stability of competitive metacommunities is insensitive to
799 dispersal connectivity in a fluctuating environment. The American Naturalist.
800 Tabi, A., T. Siqueira, and J. D. Tonkin. 2024. Species interactions drive continuous assembly of
801 freshwater communities in stochastic environments. Scientific Reports 14:21747.
802 Tatsumi, S., R. Iritani, and M. W. Cadotte. 2021. Temporal changes in spatial variation: partitioning
803 the extinction and colonisation components of beta diversity. Ecology Letters 24:1063–1072.
804 Terui, A., N. Ishiyama, H. Urabe, S. Ono, J. C. Finlay, and F. Nakamura. 2018. Metapopulation
805 stability in branching river networks. Proceedings of the National Academy of Sciences
806 115:E5963–E5969.
807 Terui, A., and J. Pomeranz. 2023. _mcbrnet: Metacommunity simulation in branching
808 networks_.
809 Tonkin, J. D., M. T. Bogan, N. Bonada, B. Rios-Touma, and D. A. Lytle. 2017. Seasonality and
810 predictability shape temporal species diversity. Ecology 98:1201–1216.
811 Vellend, M. 2016. The Theory of Ecological Communities. Edição: Mpb Series: 57 ed. Princeton
812 University Press, Princeton.
813 Vindenes, Y., and S. Engen. 2017. Demographic stochasticity and temporal autocorrelation in the
814 dynamics of structured populations.
815 https://onlinelibrary.wiley.com/doi/abs/10.1111/oik.03958.

816 Wang, S., T. Lamy, L. M. Hallett, and M. Loreau. 2019. Supp material: Stability and synchrony across
817 ecological hierarchies in heterogeneous metacommunities: linking theory to data. Ecography
818 42:1200–1211.
819 Whitlock, M. C. 2004. Selection and Drift in Metapopulations. Pages 153–173 Ecology, Genetics and
820 Evolution of Metapopulations. Elsevier.
821 Wickham, H., M. Averick, J. Bryan, W. Chang, L. McGowan, R. François, G. Grolemund, A. Hayes,
822 L. Henry, J. Hester, M. Kuhn, T. Pedersen, E. Miller, S. Bache, K. Müller, J. Ooms, D.
823 Robinson, D. Seidel, V. Spinu, K. Takahashi, D. Vaughan, C. Wilke, K. Woo, and H. Yutani.
824 2019. Welcome to the tidyverse. Journal of Open Source Software.
825 Willi, Y., J. van Buskirk, and A. A. Hoffmann. 2006. Limits to the Adaptive Potential of Small
826 Populations. Annual Review of Ecology, Evolution, and Systematics 37:433–458.
827 Xiao, J., Y. Feng, H. Zhang, C. Xu, K. Zhang, M. W. Cadotte, and L. Cheng. 2025. The proportion of
828 low abundance species is a key predictor of plant β-diversity across the latitudinal gradient.
829 Journal of Ecology 113:795–805.
830

Data availability statement: Data are already published and publicly available, with those items properly cited in this submission. Fish data are available through the iDiv Biodiversity Portal: https://doi.org/10.25829/idiv.1873-10-4000. Temperature and precipitation were obtained from TerraClimate (https://www.climatologylab.org/terraclimate.htmlv) and WorldClim (https://www.worldclim.org/). Hydrography data are available at HydroRIVERS (https://www.hydrosheds.org/products/hydrorivers) and HydroBasin https://www.hydrosheds.org/products/hydrobasins. These data and codes to reproduce results shown here can be found in Zenodo: https://doi.org/10.5281/zenodo.11242948

Table 1. Summary of fixed effects from the Gaussian location-scale GLMM modeling temporal β-diversity (rank change). The model includes ecological predictors related to local community size, environmental variability, and species richness. PL = proportion of species in the lowest abundance category. All predictors were standardized prior to model fitting. All Wald chi-square tests were performed with 1 degree of freedom. Spatial variables included to account for spatial autocorrelation in the resilduals are not shown; all were associated with P-values > 0.05, except for the second order polynomial of latitude.

Predictor	**Estimate**	**Std. Error**	**Wald χ^2**	**p-value**
Conditional Model (Mean)				
(Intercept)	0.227	0.053	–	2e-16
Local community size	–0.004	0.002	5.15	0.023
CV of community size	0.012	0.002	25.25	5.024e-07
PL	0.003	0.003	1.18	0.276
Annual mean temperature	0.045	0.018	6.19	0.013
Temperature seasonality	0.070	0.009	52.80	3.690e-13
Species richness	0.014	0.003	18.40	1.791e-05

Table 2. Summary of fixed effects from the beta regression used to model temporal variability in spatial β-diversity. The model includes ecological predictors related to community size, environmental variability, and species richness. PL = proportion of species in the lowest abundance category. All predictors were standardized prior to model fitting. All Wald chi-square tests were performed with 1 degree of freedom.

Predictor	**Estimate**	**Std. Error**	**Wald χ^2**	***p*-value**
Intercept	–2.468	0.072	–	2e-16
Metacommunity size	–0.032	0.091	0.12	0.7250
Median PL	0.010	0.108	0.01	0.9278
CV of PL	0.183	0.113	2.61	0.1059
Spatial extent	0.041	0.070	0.34	0.5620
Precipitation synchrony	–0.153	0.073	4.42	0.0356
CV of metacommunity size	0.138	0.076	3.29	0.0699
Gamma diversity	0.028	0.111	0.06	0.8020

[double column]

Figure 1. Partial effects of main predictors ($p < 0.05$) on predicted temporal variability in species composition (rank change) from the best-fitting Gaussian GLMM. (a) Local community size, (b) coefficient of variation of community size, (c) estimated species richness, (d) annual mean temperature, and (e) temperature seasonality. Shaded areas represent 95% confidence intervals. All predictors were scaled (mean = 0, SD = 1) prior to model fitting.

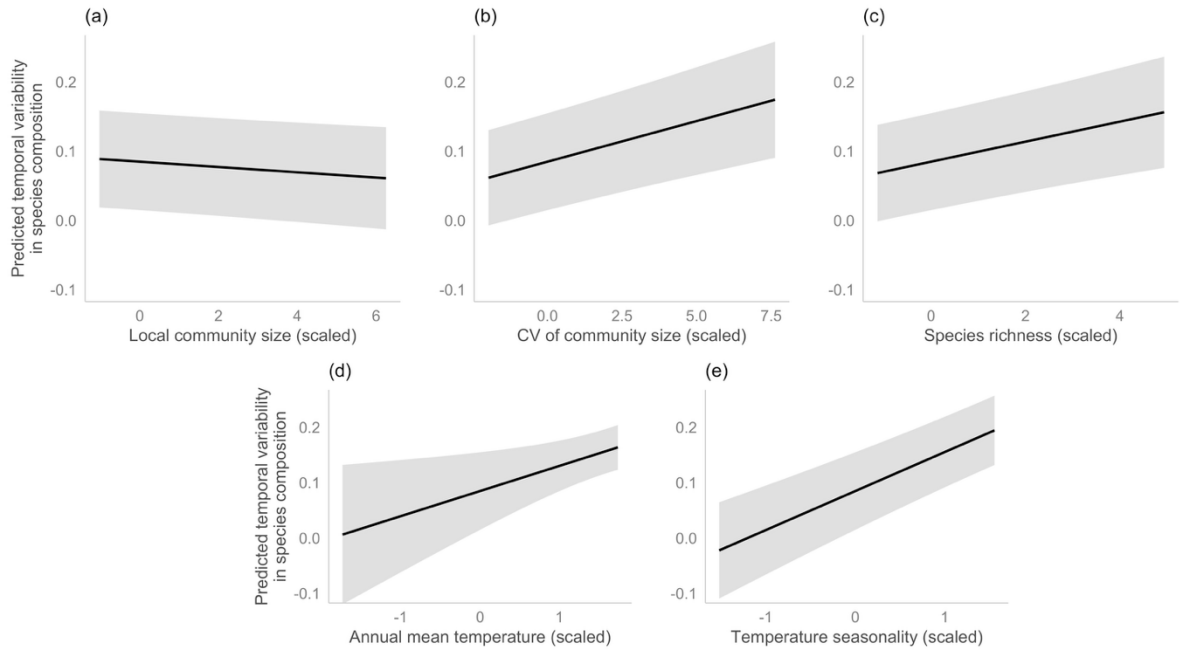
(a)
(b)
(c)
(d)
(e)
Predicted temporal variability in species composition
Local community size (scaled)
CV of community size (scaled)
Species richness (scaled)
Annual mean temperature (scaled)
Temperature seasonality (scaled)

Figure 1.

Scale-dependent shifts in demographic and environmental control of temporal β-diversity

Cristina M. Jacobi[1] & Tadeu Siqueira[1,2]

[1] Departamento de Biodiversidade, Instituto de Biociências, Universidade Estadual Paulista (UNESP), Rio Claro, SP, Brasil

[2] School of Biological Sciences, University of Canterbury, Private Bag 4800, Christchurch 8140, New Zealand, ORCID: 0000-0001-5069-290

Corresponding author: Tadeu Siqueira (tadeu.siqueira@unesp.br)

Table S1. Model selection for the analysis of temporal variability. Top: Local-scale analysis of temporal β-diversity (rank change). Bottom: Regional-scale analysis of temporal variability in spatial β-diversity (CV_rank). All models were fitted using maximum likelihood. ΔAICc represents the difference in AICc relative to the best model within each response variable group. AICc weights (AICcWt) indicate the probability that a given model is the best among the candidate set. The final selected models for each response are highlighted in bold.

Model	Description	K	AICc	ΔAICc	AICcWt	logLik
Temporal β-diversity (local scale)						
fit1_gauss	Fixed effects only (Gaussian)	9	–1201.36	174.27	0.00	609.87
fit2_gauss	+ Random intercept (hybas_id)	10	–1206.99	168.63	0.00	613.74
fit3_gauss	+ Dispersion submodel	13	–1299.12	76.50	0.00	662.96
fit3_beta	Beta distribution (full structure)	13	**–1375.63**	**0.00**	**1.00**	701.21
temp	+ Annual mean temperature	14	–1303.05	72.58	0.00	665.99
precip	+ Annual precipitation	14	–1297.86	77.77	0.00	663.39
with_seasonality	+ Temp. seasonality + Precip. seasonality	15	–1303.32	72.31	0.00	667.19
temp_range	+ Temperature annual range	14	–1302.38	73.25	0.00	665.65
precip_full	+ Annual precip. + Precip. seasonality	15	–1298.94	76.68	0.00	665.00
fit7	+ Annual mean temp. + Temp. seasonality	12	–1316.45	59.17	0.00	670.57

Model	Description	K	AICc	ΔAICc	AICcWt	logLik
fit8	+ Annual precip. + Precip. seasonality	12	–1301.87	73.76	0.00	663.28
fit9	+ Annual precip. + Temp. seasonality	12	–1297.57	78.06	0.00	661.13
fit10	+ Temp. seasonality only	11	–1299.25	76.38	0.00	660.92
best_model_spatial	+ Spatial random effect (site_id)	13	–1355.63	20.00	0.00	691.22
best_model_spatial_poly	**+ Spatial polynomials (long², lat², long:lat)**	**17**	**–1343.87**	**31.76**	**0.00**	**689.61**
best_model_spatial_poly2	+ Nested random effect (feow_id/hybas_id)	18	–1341.70	33.92	0.00	689.61
Spatial β-diversity (regional scale)						
fit1.r	**Fixed effects only (Beta, selected)**	**9**	**–138.44**	**0.00**	**0.81**	**81.33**
fit1_1.r	+ Random intercept (feow_id)	10	–134.79	3.65	0.13	81.33
fit3.r	+ Annual precip. + Precip. seasonality	11	–132.32	6.12	0.04	82.05
fit2.r	+ Dispersion submodel	13	–130.03	8.41	0.01	85.29
fit_gauss.r1	Gaussian distribution (fixed effects only)	9	–128.24	10.20	0.00	76.22
fit4.r	+ Annual precip. + Precip. seasonality + feow_id RE	12	–128.10	10.34	0.00	82.05
fit_gauss.r2	Gaussian + dispersion submodel	13	–121.53	16.91	0.00	81.05

Notes: All continuous predictors were standardized prior to model fitting. Gaussian models use identity link; Beta models use logit link. Dispersion submodels allow residual variance to vary as a function of selected predictors. Spatial polynomials include second-order terms for longitude and latitude and their interaction. ΔAICc and AICc weights are calculated relative to the best model within each response category. For temporal β-diversity, the beta model (fit3_beta) has the lowest AICc and receives 100% of the AICc weight, but the Gaussian location-scale model with spatial polynomials (best_model_spatial_poly) was selected for inference based on superior residual diagnostics and no out-of-bounds predictions. For spatial β-diversity, the beta model without random effects or dispersion submodel (fit1.r) receives 81% of the AICc weight and was selected as the final model.

Table S2. Statistics obtained in the process-based simulation model by relating the metrics of temporal variability in species composition with the median community size. Simulations were conducted using different seeds and dispersal rates. The p-value represents the significance of each relationship, and the explanatory power was measured by R^2.

Temporal variability metric	set.seed	Dispersal	Slope	p-value	R^2	Adjusted R^2
LTMC local	1234	0.1	-1.2E-04	0.0055	0.1901	0.1683
LTMC regional	1234	0.1	-6.4E-06	0.0985	0.0721	0.0470
Rank change	1234	0.1	1.0E-06	0.8411	6.3E-05	-0.0015
Rank difference	1234	0.1	1.1E-05	0.0017	0.0252	0.0227
LTMC local	1234	0.5	-3.8E-05	0.0132	0.1549	0.1321
LTMC regional	1234	0.5	-1.2E-06	0.6211	0.0067	-0.0202
Rank change	1234	0.5	8.6E-06	0.0364	0.0069	0.0053
Rank difference	1234	0.5	4.2E-06	0.301	0.0028	0.0002
LTMC local	1234	1	-3.7E-05	0.0108	0.1632	0.1406
LTMC regional	1234	1	-2.3E-06	0.405	0.0188	-0.0077
Rank change	1234	1	5.0E-07	0.9071	2.2E-05	-0.0016
Rank difference	1234	1	1.2E-05	0.0091	0.0174	0.0149
LTMC local	111	0.1	-1.3E-04	0.0001	0.328	0.3098
LTMC regional	111	0.1	-9.0E-06	0.0021	0.2274	0.2065
Rank change	111	0.1	-2.3E-07	0.9565	4.8E-06	-0.0016
Rank difference	111	0.1	1.4E-05	1.5E-06	0.0580	0.0556
LTMC local	111	0.5	-4.6E-05	0.0003	0.3016	0.2827
LTMC regional	111	0.5	-6.7E-06	0.0060	0.1868	0.1648
Rank change	111	0.5	6.3E-06	0.1187	0.0039	0.0023
Rank difference	111	0.5	2.1E-05	2.1E-08	0.0778	0.0754
LTMC local	111	1	-4.3E-05	0.0003	0.3063	0.2875
LTMC regional	111	1	-5.5E-06	0.0255	0.1278	0.1042
Rank change	111	1	-4.8E-07	0.9029	2.4E-05	-0.0016
Rank difference	111	1	1.7E-05	1.4E-05	0.0476	0.0451

Supplementary Figures

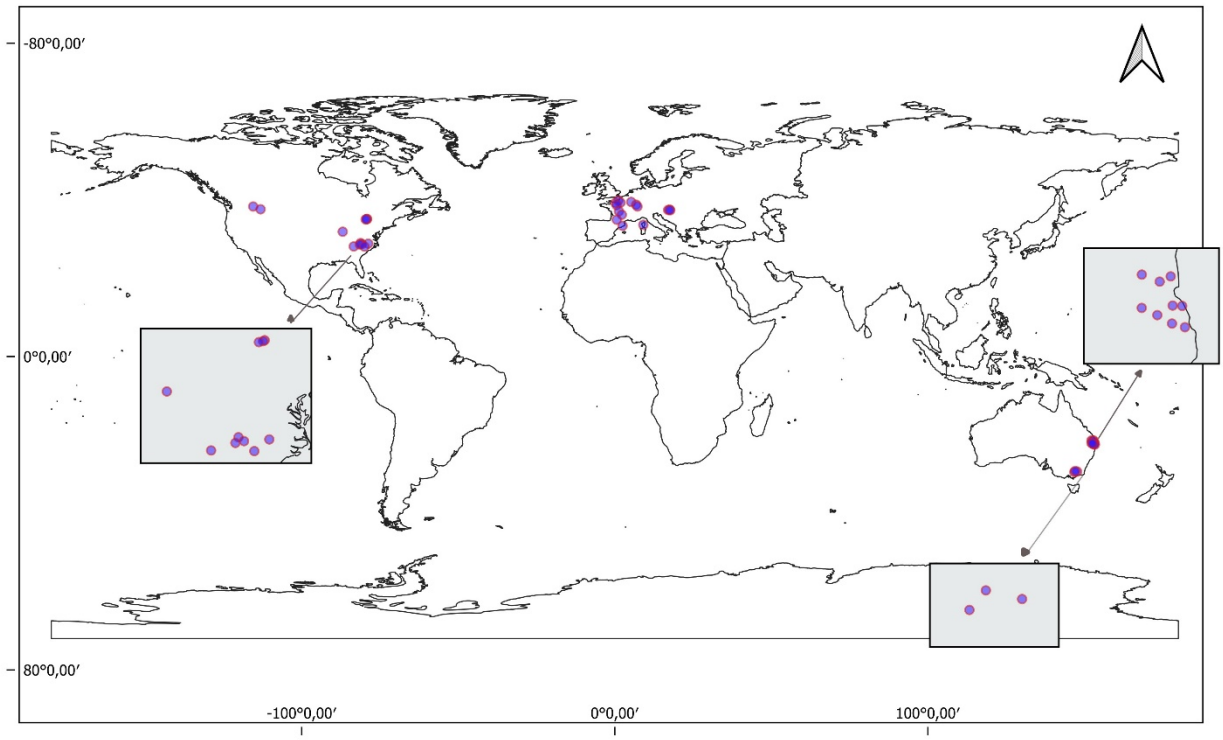

Figure S1. Geographic distribution of the 39 metacommunities selected in our study, located in Australasia (12), Nearctic (12), and Palearctic (15) biogeographical realms.

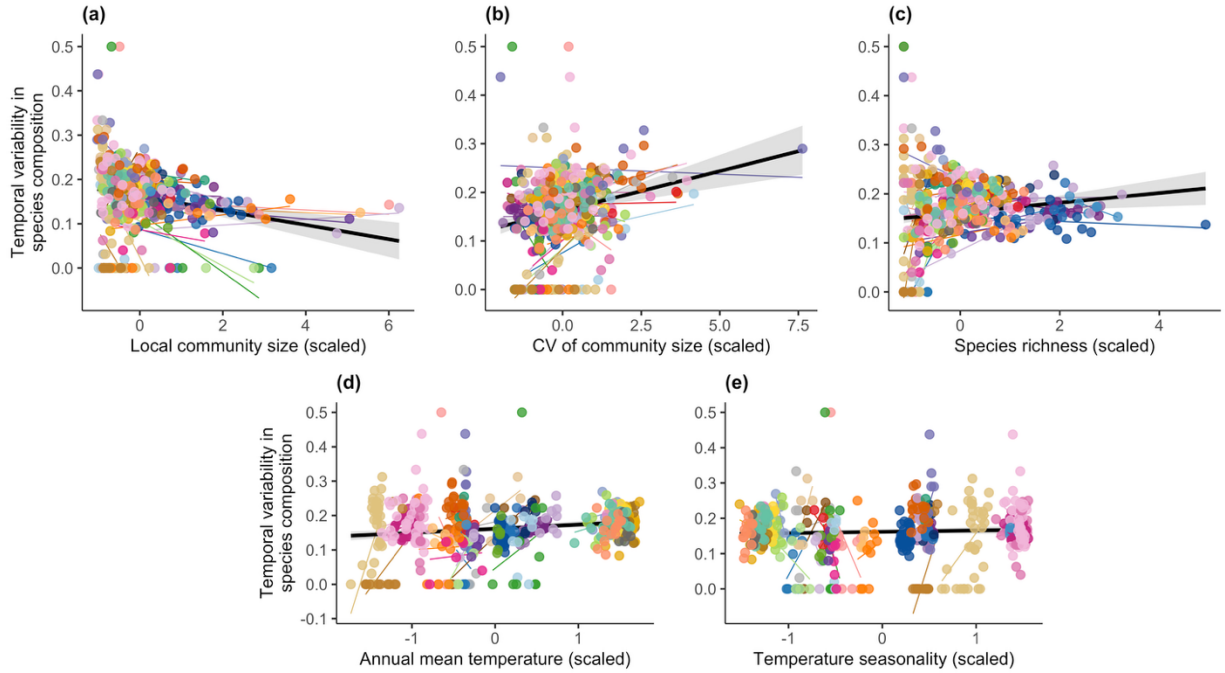

Figure S2. Raw data on temporal variability in species composition (rank change) plotted against (a) local median community size, (b) coefficient of variation (CV) of local community size, (c) estimated species richness, (d) mean annual temperature, and (e) temperature seasonality for individual metacommunities (colors). Colored lines represent basin-specific linear trends and are included as exploratory visual aids only; they are not components of the fitted model. The black line and grey ribbon represent the overall marginal relationship and its 95% confidence interval across all basins, and are also provided as exploratory visual aids only; they do not represent the conditional effects estimated by the final mixed model presented in the main text. All predictor variables were standardized prior to analysis.